Cell-free massive MIMO: Uniformly great service for everyone

Hien Quoc Ngo, Alexei Ashikhmin, Hong Yang, Erik G. Larsson and Thomas L. Marzetta

Original Publication:

Hien Quoc Ngo, Alexei Ashikhmin, Hong Yang, Erik G. Larsson and Thomas L. Marzetta, Cell-free massive MIMO: Uniformly great service for everyone, 2015, *Proceedings of the SPAWC 2015. The 16th IEEE International Workshop on Signal Processing Advances in Wireless Communications*, June 28 – July 1, 2015, Stockholm, Sweden, pp. 201-205.

Series: Signal Processing Advances in Wireless Communications, No. 2015
ISSN: 1948-3244

http://dx.doi.org/10.1109/SPAWC.2015.7227028

Cell-Free Massive MIMO: Uniformly Great Service For Everyone

Hien Quoc Ngo*, Alexei Ashikhmin†, Hong Yang†, Erik G. Larsson*, and Thomas L. Marzetta†
*Department of Electrical Engineering (ISY), Linköping University, 581 83 Linköping, Sweden
†Bell Laboratories, Alcatel-Lucent, Murray Hill, NJ 07974, USA

***Abstract*—We consider the downlink of Cell-Free Massive MIMO systems, where a very large number of distributed access points (APs) simultaneously serve a much smaller number of users. Each AP uses local channel estimates obtained from received uplink pilots and applies conjugate beamforming to transmit data to the users. We derive a closed-form expression for the achievable rate. This expression enables us to design an optimal max-min power control scheme that gives equal quality of service to all users.**

We further compare the performance of the Cell-Free Massive MIMO system to that of a conventional small-cell network and show that the throughput of the Cell-Free system is much more concentrated around its median compared to that of the small-cell system. The Cell-Free Massive MIMO system can provide an almost $20-$fold increase in 95%-likely per-user throughput, compared with the small-cell system. Furthermore, Cell-Free systems are more robust to shadow fading correlation than small-cell systems.

I. Introduction

In Massive MIMO, large collocated or distributed antenna arrays are deployed at wireless base stations [1]. Collocated Massive MIMO architectures, where all service antennas are located in a compact area, have the advantage that the backhaul requirements are low. By contrast, in distributed Massive MIMO, the service antennas are spread out over a wide area. Owing to its ability to fully exploit macro-diversity and differences in path loss, distributed Massive MIMO can potentially offer a very high probability of coverage. At the same time, it can offer all the advantages of collocated Massive MIMO. Despite its potential, however, fairly little work on distributed Massive MIMO is available in the literature. Some comparisons between distributed and collocated systems were performed in [2] for the uplink and in [3], [4] for the downlink. In [3], [4], perfect channel state information was assumed to be available both at the base station and at the users.

On a parallel avenue, small-cell systems, where the base stations do not cooperate coherently, are often viewed as enablers for high spectral efficiency and coverage [5]. However, a comparison between small-cell and distributed Massive MIMO is not yet available.

Contribution of the paper: We consider a distributed Massive MIMO system where a large number of service antennas, called access points (APs), and a much smaller number of autonomous users are distributed at random over a wide area. All APs cooperate via a backhaul network, and serve all users in the same time-frequency resource via time-division duplex (TDD) operation. There are no cells or cell boundaries. Hence, we call this system "Cell-Free Massive MIMO". Cell-Free Massive MIMO is expected to offer many advantages: 1) a huge throughput, coverage probability and energy efficiency; and 2) averaging out of small-scale fading and uncorrelated noise so that the performance depends only on the large-scale fading. In this paper, we restrict the discussion to the downlink of Cell-Free systems with conjugate beamforming. We assume that the channels are estimated through uplink pilots. The paper makes the following specific contributions:

- We derive a closed-form expression for the achievable rate with a finite number of APs, taking into account channel estimation errors, power control, and the non-orthogonality of pilot sequences. In [6], corresponding capacity bounds were derived assuming pilot sequences are orthogonal.
- We design two pilot assignment schemes: *random pilot assignment* and *greedy pilot assignment*. We show that the greedy pilot assignment is better.
- We propose a max-min power control algorithm that maximizes the smallest of all user rates, under a per-AP power constraint. This power control problem is formulated as a quasi-convex optimization problem.
- We compare the performance of Cell-Free Massive MIMO and conventional small-cell systems under uncorrelated and correlated shadowing models. Conclusions of this comparison are given in Section VI.

II. System Model

We consider a network of M APs that serve K users in the same time-frequency resource. All APs and users are equipped with a single antenna, and they are randomly located in a large area. In this work, we consider the downlink with conjugate beamforming. We consider only the conjugate beamforming technique since it is simple and can be implemented in a distributed manner. The transmission from the APs to the users proceed by TDD operation, including two phases for each coherence interval: uplink training and downlink payload data transmission. In the uplink training phase, the users send pilot sequences to the APs and each AP estimates its own CSI. This is performed in a decentralized fashion. The so-obtained channel estimates are used to precode the transmit signals.

A. Uplink Training

Let T be the length of the coherence interval (in samples), and let τ be the length of uplink training duration (in samples) per coherence interval. It is required that $\tau < T$. During the training phase, all K users simultaneously send pilot

sequences of length τ samples to the APs. Let $\boldsymbol{\varphi}_k \in \mathbb{C}^{\tau \times 1}$, where $\|\boldsymbol{\varphi}_k\|^2 = 1$, be the pilot sequence used by the kth user. Then, the $\tau \times 1$ pilot vector received at the mth AP is

$$\mathbf{y}_m = \sqrt{\tau \rho_{\mathrm{p}}} \sum_{k=1}^{K} g_{mk} \boldsymbol{\varphi}_k + \mathbf{w}_m, \tag{1}$$

where ρ_{p} is the normalized transmit signal-to-noise ratio (SNR) of each pilot symbol, $\mathbf{w}_m$ is a vector of additive noise at the mth AP—whose elements are i.i.d. $\mathcal{CN}(0,1)$ random variables (RVs), and g_{mk} denotes the channel coefficient between the kth user and the mth AP. The channel g_{mk} is modeled as follows:

$$g_{mk} = \beta_{mk}^{1/2} h_{mk}, \tag{2}$$

where h_{mk} represents the small-scale fading, and β_{mk} represents the path loss and large-scale fading. We assume that h_{mk}, $m = 1, \ldots, M$, $k = 1, \ldots K$, are i.i.d. $\mathcal{CN}(0,1)$ RVs.

Based on the received pilot signal $\mathbf{y}_m$, the mth AP will estimate the channel $g_{mk}, \forall k = 1, ..., K$. Let $\tilde{y}_{mk} \triangleq \boldsymbol{\varphi}_k^H \mathbf{y}_m$ be the projection of $\mathbf{y}_m$ on $\boldsymbol{\varphi}_k^H$:

$$\tilde{y}_{mk} = \sqrt{\tau \rho_{\mathrm{p}}} g_{mk} + \sqrt{\tau \rho_{\mathrm{p}}} \sum_{\substack{k'=1 \\ k' \neq k}}^{K} g_{mk'} \boldsymbol{\varphi}_k^H \boldsymbol{\varphi}_{k'} + \boldsymbol{\varphi}_k^H \mathbf{w}_m. \tag{3}$$

Although, for arbitrary pilot sequences, $\tilde{y}_{mk}$ is not a sufficient statistic for the estimation of g_{mk}, one can still use this quantity to obtain suboptimal estimates. In the case where any pair of pilot sequences is either fully correlated or exactly orthogonal, then $\tilde{y}_{mk}$ is a sufficient statistic, and estimates based on $\tilde{y}_{mk}$ are optimal. The MMSE estimate of g_{mk} given $\tilde{y}_{mk}$ is

$$\hat{g}_{mk} = \frac{\sqrt{\tau \rho_{\mathrm{p}}} \beta_{mk} \tilde{y}_{mk}}{\tau \rho_{\mathrm{p}} \sum_{k'=1}^{K} \beta_{mk'} \left| \boldsymbol{\varphi}_k^H \boldsymbol{\varphi}_{k'} \right|^2 + 1}. \tag{4}$$

Remark 1: If $\tau \geq K$, then we can choose $\boldsymbol{\varphi}_1, \boldsymbol{\varphi}_2, \cdots, \boldsymbol{\varphi}_K$ so that they are pairwisely orthogonal, and hence, the second term in (3) disappears. Then the channel estimate $\hat{g}_{mk}$ is independent of $g_{mk'}$, $k' \neq k$. However, owing to the limited length of the coherence interval, in general, $\tau < K$, and non-orthogonal pilot sequences must be used by different users. The channel estimate $\hat{g}_{mk}$ is degraded by pilot signals transmitted from other users (the second term in (3)). This causes the so-called pilot contamination effect. There is still room for a considerable number of orthogonal pilots. For the case of pedestrians with mobility less than 3 km/h, at a 2 GHz carrier frequency the product of the coherence bandwidth and the coherence time is equal to $17,640$ (assuming a delay spread of 4.76 μs) [7], so if half of the coherence time is utilized for pilots then there is an available pool of 8820 mutually orthogonal pilots.

B. Downlink Payload Data Transmission

The APs treat the channel estimates as the true channels, and use conjugate beamforming to transmit signals to the K users. Let s_k, $k = 1, \ldots, K$, where $\mathbb{E}\{|s_k|^2\} = 1$, be the symbol intended for the kth user. With conjugate beamforming, the transmitted signal from the mth AP is

$$x_m = \sqrt{\rho_{\mathrm{d}}} \sum_{k=1}^{K} \eta_{mk}^{1/2} \hat{g}_{mk}^* s_k, \tag{5}$$

where η_{mk}, $m = 1, \ldots, M$, $k = 1, \ldots K$, are power control coefficients chosen to satisfy the following average power constraint at each AP:

$$\mathbb{E}\{|x_m|^2\} \leq \rho_{\mathrm{d}}. \tag{6}$$

With the channel model in (2), the power constraint $\mathbb{E}\{|x_m|^2\} \leq \rho_{\mathrm{d}}$ can be rewritten as:

$$\sum_{k=1}^{K} \eta_{mk} \gamma_{mk} \leq 1, \tag{7}$$

where

$$\gamma_{mk} \triangleq \mathbb{E}\left\{ |\hat{g}_{mk}|^2 \right\} = \frac{\tau \rho_{\mathrm{p}} \beta_{mk}^2}{\tau \rho_{\mathrm{p}} \sum_{k'=1}^{K} \beta_{mk'} \left| \boldsymbol{\varphi}_k^H \boldsymbol{\varphi}_{k'} \right|^2 + 1}. \tag{8}$$

The received signal at the kth user is given by

$$r_k = \sum_{m=1}^{M} g_{mk} x_m + n_k = \sqrt{\rho_{\mathrm{d}}} \sum_{m=1}^{M} \sum_{k'=1}^{K} \eta_{mk'}^{1/2} g_{mk} \hat{g}_{mk'}^* s_{k'} + n_k, \tag{9}$$

where n_k represents additive Gaussian noise at the kth user. We assume that $n_k \sim \mathcal{CN}(0,1)$. Then s_k will be detected from r_k.

III. Achievable Rate

In this section, we derive a closed-form expression for the achievable rate, using similar analysis techniques as in [8]. We assume that each user has knowledge of the channel statistics but not of the channel realizations. The received signal r_k in (9) can be rewritten as

$$r_k = \mathtt{DS}_k \cdot s_k + \mathtt{EN}_k, \tag{10}$$

where $\mathtt{DS}_k \triangleq \sqrt{\rho_{\mathrm{d}}}\, \mathbb{E}\left\{ \sum_{m=1}^{M} \eta_{mk}^{1/2} g_{mk} \hat{g}_{mk}^* \right\}$ is a deterministic factor that scales the desired signal, and $\mathtt{EN}_k$ is an "effective noise" term which equals the RHS of (9) minus $\mathtt{DS}_k \cdot s_k$. A straightforward calculation shows that the effective noise and the desired signal are uncorrelated. Therefore, by using the fact that uncorrelated Gaussian noise represents the worst case, we obtain the following achievable rate of the kth user for Cell-Free (cf) operation:

$$R_k^{\mathrm{cf}} = \log_2 \left(1 + \frac{|\mathtt{DS}_k|^2}{\mathbb{V}\mathrm{ar}\{\mathtt{EN}_k\}} \right). \tag{11}$$

We next provide a new exact closed-form expression for the achievable rate given by (11), for a finite number of APs. (The proof is omitted due to space constraints.)

Theorem 1: An achievable rate of the transmission from the APs to the kth user is given by (12), shown at the top of the next page.

$$R_k^{\text{cf}} = \log_2\left(1 + \frac{\rho_{\text{d}}\left(\sum_{m=1}^{M}\eta_{mk}^{1/2}\gamma_{mk}\right)^2}{\rho_{\text{d}}\sum_{k'\neq k}^{K}\left(\sum_{m=1}^{M}\eta_{mk'}^{1/2}\gamma_{mk'}\frac{\beta_{mk}}{\beta_{mk'}}\right)^2|\boldsymbol{\varphi}_{k'}^H\boldsymbol{\varphi}_k|^2 + \rho_{\text{d}}\sum_{k'=1}^{K}\sum_{m=1}^{M}\eta_{mk'}\gamma_{mk'}\beta_{mk} + 1}\right). \quad (12)$$

IV. Pilot Assignment and Power Control

In this section, we will present methods to assign the pilot sequences to the users, and to control the power. Note that pilot assignment and power control are decoupled problems because the pilots are not power controlled.

A. Pilot Assignment

As discussed in Remark 1, non-orthogonal pilot sequences must be used by different users due to the limited length of the coherence interval. The main question is how the pilot sequences should be assigned to the K users. In the following, we present two simple pilot assignment schemes.

1) Random Pilot Assignment: Since the length of the pilot sequences is τ, we can have τ orthogonal pilot sequences. With random pilot assignment, each user will be randomly assigned one pilot sequence from the set of τ orthogonal pilot sequences.

This random pilot assignment method is simple. However, with high probability, two users that are in close vicinity of each other will use the same pilot sequence. As a result, the performance of these users is not good, due to the high pilot contamination effect.

2) Greedy Pilot Assignment: Next we propose a simple greedy pilot assignment method, that addresses the shortcomings of random pilot assignment. With greedy pilot assignment, the K users are first randomly assigned K pilot sequences. Then the worst-user (with lowest rate), say user k, updates its pilot sequence so that its pilot contamination effect is minimized. The algorithms then proceeds iteratively.

The pilot contamination effect at the kth user is reflected by the second term in (3) which has variance $\sum_{k'\neq k}^{K}\beta_{mk'}\left|\boldsymbol{\varphi}_k^H\boldsymbol{\varphi}_{k'}\right|^2$. So, the worst-user (the kth user) will find a new pilot sequence which minimizes the pilot contamination, summed over all APs:

$$\arg\min_{\boldsymbol{\varphi}_k}\sum_{m=1}^{M}\sum_{k'\neq k}^{K}\beta_{mk'}\left|\boldsymbol{\varphi}_k^H\boldsymbol{\varphi}_{k'}\right|^2. \quad (13)$$

Since $\|\boldsymbol{\varphi}_k\|^2 = 1$, the expression in (13) is a Rayleigh quotient, and hence, the updated pilot sequence of the kth user is the eigenvector which corresponds to the smallest eigenvalue of the matrix $\sum_{m=1}^{M}\sum_{k'\neq k}^{K}\beta_{mk'}\boldsymbol{\varphi}_{k'}\boldsymbol{\varphi}_{k'}^H$.

B. Power Control

In our work, we focus on max-min power control. Specifically, given realizations of the large-scale fading, we find the power control coefficients η_{mk}, $m = 1,\cdots,M, k = 1,\cdots,K$, which maximize the minimum of the rates of all users, under the power constraint (7):

$$\begin{aligned}\max_{\{\eta_{mk}\}} \quad & \min_{k=1,\cdots,K} R_k^{\text{cf}} \\ \text{subject to} \quad & \textstyle\sum_{k=1}^{K}\eta_{mk}\gamma_{mk} \leq 1,\ m = 1,...,M \\ & \eta_{mk} \geq 0,\ k = 1,...,K,\ m = 1,...,M.\end{aligned} \quad (14)$$

Define $\varsigma_{mk} \triangleq \eta_{mk}^{1/2}$. Then, by introducing the slack variables $\varrho_{k'k}$ and ϑ_m, and using (12), we can reformulate (14) as

$$\begin{aligned}\max_{\{\varsigma_{mk},\varrho_{k'k},\vartheta_m\}} \quad & \min_{k=1,\cdots,K} \frac{\left(\sum_{m=1}^{M}\gamma_{mk}\varsigma_{mk}\right)^2}{\sum_{k'\neq k}^{K}|\boldsymbol{\varphi}_{k'}^H\boldsymbol{\varphi}_k|^2\varrho_{k'k}^2 + \sum_{m=1}^{M}\beta_{mk}\vartheta_m^2 + \frac{1}{\rho_{\text{d}}}} \\ \text{subject to} \quad & \textstyle\sum_{k'=1}^{K}\gamma_{mk'}\varsigma_{mk'}^2 \leq \vartheta_m^2,\ m = 1,...,M \\ & \textstyle\sum_{m=1}^{M}\gamma_{mk'}\frac{\beta_{mk}}{\beta_{mk'}}\varsigma_{mk'} \leq \varrho_{k'k},\ \forall k' \neq k \\ & 0 \leq \vartheta_m \leq 1,\ m = 1,...,M \\ & \varsigma_{mk} \geq 0,\ k = 1,...,K,\ m = 1,...,M.\end{aligned} \quad (15)$$

We then have the following result. (The proof is omitted due to space constraints.)

Proposition 1: The optimization problem (15) is quasi-concave.

Since the optimization problem (15) is quasi-concave, it can be solved efficiently by using bisection and solving a sequence of convex feasibility problems [9].

V. Numerical Results and Discussions

We provide some numerical results on Cell-Free Massive MIMO performance. The M APs and K users are uniformly distributed at random within a square of size 1000×1000 m^2. The coefficient β_{mk} models the path loss and shadow fading, according to

$$\beta_{mk} = \text{PL}_{mk} \cdot 10^{\frac{\sigma_{\text{sh}}z_{mk}}{10}}, \quad (16)$$

where PL_{mk} represents path loss, and $10^{\frac{\sigma_{\text{sh}}z_{mk}}{10}}$ represents shadow fading with standard deviation σ_{sh}, and $z_{mk} \sim \mathcal{N}(0,1)$. We use a three-slope model for the path loss [10]: the path loss exponent equals 3.5 if the distance between the mth AP and the kth user (denoted by d_{mk}) is greater than d_1, equals 2 if $d_1 \geq d_{mk} > d_0$, and equals 0 if $d_{mk} \leq d_0$. To determine the path loss in absolute numbers, we employ the Hata-COST231 propagation model for $d_{mk} > d_1$.

In all examples, we choose the following parameters: the carrier frequency is 1.9 GHz, the AP radiated power is 200 mW, the noise figure (uplink and downlink) is 9 dB, the AP antenna height is 15 m, the user antenna height is 1.65 m, $\sigma_{\text{sh}} = 8$ dB, $d_1 = 50$, and $d_0 = 10$ m. To avoid boundary effects, and to imitate a network with infinite area, the square area is wrapped around.

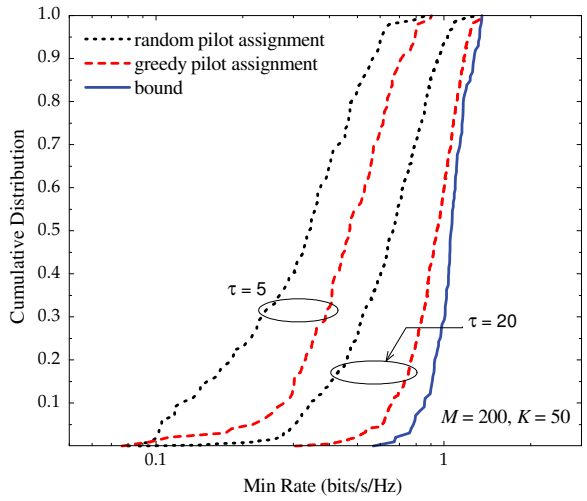

Fig. 1. The minimum per-user rate for different τ, without power control. Here, $M = 200$, $K = 50$, and $D = 1$ km.

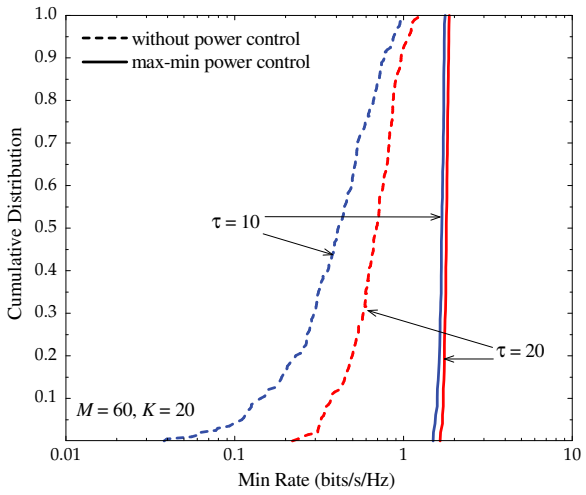

Fig. 2. The minimum rates without power control and with max-min power control. Here, $M = 60$, $K = 20$, and $\tau = 10$ and 20.

A. Pilot Assignment

We first examine the performance of Cell-Free Massive MIMO with different pilot assignment schemes, assuming that no power control is performed. Without power control, all APs transmit with full power, $\eta_{mk} = \eta_{mk'}$, $\forall k = 1, \ldots K$. Figure 1 shows the cumulative distribution of the minimum per-user rate, for $M = 200$, and $K = 50$, and for different τ. The "bound" curve shows the case where all K users are assigned orthogonal pilot sequences, so there is no pilot contamination. As expected, when τ increases, the pilot contamination effect reduces, and hence, the rate increases. We can see that when $\tau = 20$, then by using greedy pilot assignment the 95%-likely minimum rate can be doubled as compared to when random pilot assignment is used. In addition, even when τ is very small ($\tau = 5$), Cell-Free Massive MIMO still provides good service for all users. More importantly, the gap between the performance of greedy pilot assignment and the bound is not significant. Hence, the greedy pilot assignment scheme is fairly good and henceforth this is the method we will use.

B. Max-Min Power Control

In the following, we will examine effectiveness of the max-min power control. Fig. 2 shows the the cumulative distribution of the achievable rates with max-min and no power control respectively, for $M = 60$, $K = 20$, and $\tau = 10, 20$. We can see that with max-min power control, the system performance improves significantly. When $\tau = 10$, the max-min power allocation can improve the 95%-likely rate by a factor of 15 compared to the case of without power control. In addition, by using power control, the effect of pilot contamination can be notably reduced.

C. Cell-Free Massive MIMO versus Small-Cell Systems

Next we compare the performance of Cell-Free Massive MIMO to that of small-cell systems.

1) Small-Cell Systems: To model a small-cell system, we assume that each user is served by exactly one AP. For a given user, the available AP with the largest average received power is selected. Once an AP is chosen by some user, this AP then becomes unavailable. Mathematically, we let m_k be the AP chosen by the kth user:

$$m_k \triangleq \underset{m \in \{\text{available APs}\}}{\arg\max} \beta_{mk}.$$

In small-cell operation, the users estimate the channels. Let $\boldsymbol{\varphi}_{m_k} \in \mathbb{C}^{\tau \times 1}$ be the pilot sequence transmitted from the m_kth AP, and let ρ_{p} be the average transmit power per pilot symbol. We assume that the APs transmit with full power. Similarly to the derivation of Cell-Free Massive MIMO (details omitted due to space constraints), we can derive an achievable rate for the kth user in a small-cell system as:

$$R_k^{\mathrm{sc}} = \mathbb{E}\left\{ \log_2\left(1 + \frac{\rho_{\mathrm{d}} \left|\hat{g}_{m_k k}\right|^2}{\rho_{\mathrm{d}}(\beta_{m_k k} - \gamma_{m_k k}) + \rho_{\mathrm{d}} \sum\limits_{k' \neq k}^{K} \beta_{m_{k'} k} + 1}\right)\right\},$$

where $\hat{g}_{m_k k} \sim \mathcal{CN}(0, \gamma_{m_k k})$ is the MMSE channel estimate of $g_{m_k k}$ at the kth user, and $\gamma_{m_k k}$ is given by (8).

2) Spatial Shadowing Correlation Models: Transmitters/receivers that are in close vicinity of each other will experience correlated shadow fading. Next, we investigate the effect of shadowing correlation on both small-cell and Cell-Free Massive MIMO systems.

Most existing correlation models for the shadow fading model two correlation effects from the user perspective: cross-correlation and spatial correlation [11]. The cross-correlation effect represents the correlation between the shadowing coefficients from different base stations to a given user. The spatial correlation effect represents the correlation due to the relative positions between the users. This model neglects the effects of cross-correlation and spatial correlation from the base station sides. Doing so is reasonable when the base station antennas

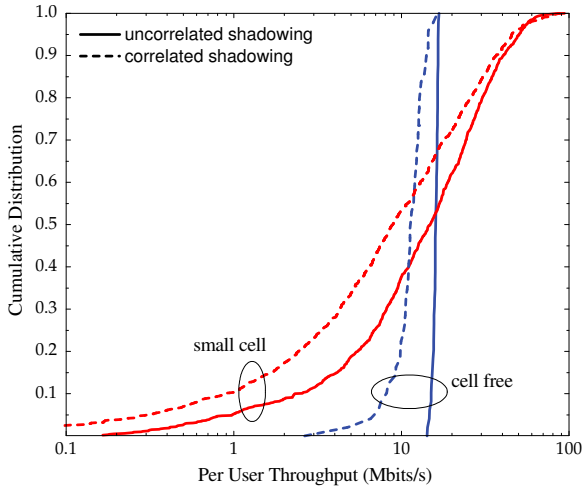

Fig. 3. The cumulative distribution of the throughput per user for correlated and uncorrelated shadow fading. Here, $M = 60$, $K = 20$, and $\tau = 10$.

are located high above the ground, and all base stations are well separated. However, in our system models, both the APs and the users are located randomly in the network, and they may be close to each other. In addition, the AP antenna elevation is not very high. Hence, the correlation at the AP side should be taken into account as well. We will use the following modified correlation model for the shadow fading:

$$z_{mk} = \sqrt{\rho_1} a_m + \sqrt{1-\rho_1} b_k, \;\; m = 1, \ldots, M, \;\; k = 1, \ldots, K,$$

where $a_m \sim \mathcal{N}(0,1)$ and $b_k \sim \mathcal{N}(0,1)$ are independent. The quantity ρ_1 ($0 \leq \rho_1 \leq 1$) represents the cross-correlation at the AP side, and $1-\rho_1$ represents the cross-correlation at the user side. The spatial correlation is reflected via the correlation between a_m, $m = 1, \ldots, M$, and the correlation between b_k, $k = 1, \ldots, K$. We define $\rho_{2,mm'} \triangleq \mathbb{E}\{a_m a_{m'}^*\}$ and $\rho_{3,kk'} \triangleq \mathbb{E}\{b_k b_{k'}^*\}$. These correlation coefficients depend on the spatial locations of the APs and on the users:

$$\rho_{2,mm'} = 2^{-\frac{d_{\mathrm{a}}(m,m')}{d_{\mathrm{decorr}}}}, \quad \rho_{3,kk'} = 2^{-\frac{d_{\mathrm{u}}(k,k')}{d_{\mathrm{decorr}}}}, \qquad (17)$$

where $d_{\mathrm{a}}(m,m')$ is the distance between the mth and m'th APs, $d_{\mathrm{u}}(k,k')$ is the distance between the kth and k'th users, and d_{decorr} is the decorrelation distance which depends on the environment. This model for the correlation coefficients has been validated by practical experiments [11].

For the comparison between Cell-Free Massive MIMO and small-cell systems, we consider the per-user throughput which is defined as:

$$S_k^{\mathtt{A}} = B \frac{1-\tau/T}{2} R_k^{\mathtt{A}},$$

where $\mathtt{A} \in \{\mathrm{cf}, \mathrm{sc}\}$ corresponding to Cell-Free Massive MIMO and small-cell systems respectively, B is the spectral bandwidth, and T in the length of the coherence interval in samples. Note that both Cell-Free Massive MIMO and small-cell systems need K pilot sequences for the channel estimation. There is no difference between Cell-Free Massive MIMO and small-cell systems in terms of pilot overhead. Therefore, we assume that both systems use the same set of pilot sequences. We choose $T = 200$ samples, $B = 20$ MHz, $d_{\mathrm{decorr}} = 0.1$ km and $\rho_1 = 0.5$.

Figure 3 compares the cumulative distribution of the throughput per user for small-cell and Cell-Free systems, for $M = 60$, $K = 20$, and $\tau = 10$, with and without shadow fading correlation. Compared to the small-cell systems, the throughput of the Cell-Free systems is much more concentrated around its median. Without shadow fading correlation, the 95%-likely throughput of the Cell-Free system is about 15 Mbits/s which is 17 times higher than that of the small-cell system (about 0.85 Mbits/s). We can see that the small-cell systems are more affected by shadow fading correlation than the Cell-Free Massive MIMO systems are. In this example, the shadow fading correlation reduces the 95%-likely throughput by factors of 4 and 2 for small-cell and Cell-Free systems, respectively, compared to the case of uncorrelated shadowing.

VI. Conclusion

We analyzed the performance of Cell-Free Massive MIMO systems, taking into account the effects of channel estimation. We further compared the performance of Cell-Free Massive MIMO to that of small-cell systems.

The results show that Cell-Free systems can significantly outperform small-cell systems in terms of throughput. The 95%-likely per-user throughput of Cell-Free Massive MIMO is almost 20 times higher than for a small-cell system. Also, Cell-Free Massive MIMO systems are more robust to shadow fading correlation than small-cell systems.

References

[1] E. G. Larsson, F. Tufvesson, O. Edfors, and T. L. Marzetta, "Massive MIMO for next generation wireless systems," *IEEE Commun. Mag.*, vol. 52, no. 2, pp. 186–195, Feb. 2014.

[2] K. T. Truong and R. W. Heath Jr., "The viability of distributed antennas for massive MIMO systems," in *Proc. 45th Asilomar Conference on Signals, Systems and Computers (ACSSC '06)*, Pacific Grove, CA, USA, Nov. 2013, pp. 1318–1323.

[3] Z. Li and L. Dai, "A comparative study of downlink MIMO cellular networks with co-located and distributed base-station antennas," *IEEE Trans. Commun.*, 2014, submitted. [Online]. Available: hhttp://arxiv.org/abs/1401.1203

[4] K. Hosseini, W. Yu, and R. S. Adve, "Large-scale MIMO versus network MIMO for multicell interference mitigation," *IEEE J. Select. Topics Signal Process.*, vol. 8, no. 5, pp. 930–941, Oct. 2014.

[5] W. Liu, S. Han, C. Yang, and C. Sun, "Massive MIMO or small cell network: Who is more energy efficient?" in *Proc. IEEE WCNC 2013 workshop on n Future Green End-to-End wireless Network*, Shanghai, China, 2013, pp. 24–29.

[6] H. Yang and T. L. Marzetta, "Capacity performance of multicell large scale antenna systems," in *Proc. 51st Allerton Conference on Communication, Control, and Computing*, Urbana-Champaign, Illinois, Oct. 2013.

[7] D. N. C. Tse and P. Viswanath, *Fundamentals of Wireless Communications*. Cambridge, UK: Cambridge University Press, 2005.

[8] B. Hassibi and B. M. Hochwald, "How much training is needed in multiple-antenna wireless links?" *IEEE Trans. Inf. Theory*, vol. 49, no. 4, pp. 951–963, Apr. 2003.

[9] S. Boyd and L. Vandenberghe, *Convex Optimization*. Cambridge, UK: Cambridge University Press, 2004.

[10] A. Tang, J. Sun, and K. Gong, "Mobile propagation loss with a low base station antenna for NLOS street microcells in urban area," in *Proc. IEEE Veh. Technol. Conf. (VTC)*, May 2001, pp. 333–336.

[11] Z. Wang, E. K. Tameh, and A. R. Nix, "Joint shadowing process in urban peer-to-peer radio channels," *IEEE Trans. Veh. Technol.*, vol. 57, no. 1, pp. 52–64, Jan. 2008.